CELL CYCLE
2018, VOL. 17, NO. 18, 2309–2320
https://doi.org/10.1080/15384101.2018.1535219

Taylor & Francis
Taylor & Francis Group

RESEARCH PAPER

Role of AhR in regulating cancer stem cell–like characteristics in choriocarcinoma

Chenchun Wu, Shuran Yu, Qianxia Tan, Peng Guo, and Huining Liu

Department of Gynecology and Obstetrics, Xiangya Hospital Central South University, Changsha, Hunan, China

ABSTRACT

Choriocarcinoma is sensitive to chemotherapy. However, drug resistance has become one of the major problems in recent years. Previous studies have shown that many tumors contained a small fraction of cells that exhibited enhanced tumor initiating potential and stem cell-like properties. It is hypothesized that cancer stem cells (CSCs) are organized in a cellular hierarchy. They also have the qualities of self-renewal, chemoresistance, and so on. The identification of CSCs in choriocarcinoma and the mechanism contributing to their qualities remain largely unknown. This study focused on the role of AhR, a transcription factor abundantly expressed in many different types of cancer, in the regulation of the expansion of choriocarcinoma CSCs and the exact molecular mechanisms. Spheroid cells isolated from choriocarcinoma in serum-free conditions have stem cell–like characteristics. The expression and nuclear translocation of AhR were markedly elevated in spheroid cells. Activation of AhR by 2,3,7,8-tetrachlorodibenzo-*p*-dioxin (TCDD) significantly increased the spheroid-forming efficiency, chemotherapy resistance, and ability to form tumor xenografts of the cells, whereas AhR knockdown, using short hairpin RNA (shRNA), dramatically reduced stem cell properties. Mechanistically, activating the β-catenin pathway might be an essential biological function of AhR during the regulation of the CSC characteristics. This study also identified ABCG2, which plays an important role in CSCs, as a direct target of AhR. Together, these results strongly suggested the participation of AhR in choriocarcinoma carcinogenesis. Targeting AhR may provide a novel therapeutic opportunity for choriocarcinoma.

ARTICLE HISTORY
Received 19 February 2018
Revised 6 September 2018
Accepted 3 October 2018

KEYWORDS
Choriocarcinoma; stem cell; AhR

Introduction

Choriocarcinoma is a malignant disorder of gestational trophoblastic disease. It is characterized by abnormal proliferation of human chorionic gonadotropin–producing trophoblasts. Early metastasis is commonly observed in choriocarcinoma. Despite its aggressiveness, about 100% of low-risk and 84% of high-risk patients with gestational trophoblastic neoplasia, which is highly sensitive to chemotherapy [1], are cured from the tumor. The cure rate of choriocarcinoma and metastatic choriocarcinoma is 80% and about 75%, respectively [2,3]. However, drug resistance in chemotherapy has been reported in recent years, leading to poor outcomes in the clinic, such as recurrence, loss of fertility, or ultimately death [4–6]. Therefore, the mechanism underlying choriocarcinoma invasion and resistance needs to be investigated.

Bonnet et al. identified cancer stem cells (CSCs) in myeloid leukemia for the first time [7]. In 2006, CSCs were defined as "cells within a tumor that possess the capacity for self-renewal and can cause the heterogeneous lineages of cancer cells that constitute the tumor" in the Cancer Stem Cell Workshop of the AACR [8]. Furthermore, CSCs were identified in most solid tumors, including breast cancer, brain cancer, and many other types of cancer [9–12]. The characteristics of CSCs include high capacity to form tumor spheres and high levels of ATP-binding cassette drug transporters (particularly ABCG2) [13,14]. Moreover, the CSC biology is controlled by several signaling pathways such as the Wnt pathway. The Wnt pathway is known to mediate CSC self-renewal by modulating the transcription factor β-catenin [15]. The hypothesis that tumor cells are driven by CSCs has provided clues that CSCs can be considered as an important target for cancer treatment and prevention [16].

AhR is a ligand-activated member of the basic helix-loop-helix/Per-ARNT-Sim (bHLH-PAS) family of transcriptional factors, all of which are important in biological functions [17]. Recent studies suggest that

CONTACT Huining Liu liuhuining@csu.edu.cn
Supplemental data for this article can be accessed here.

AhR, which is chronically active in several cancers, is involved in regulating cell proliferation, invasion, migration, and cancer imitation [18,19]. Activation of AhR by binding to 2,3,7,8-tetrachlorodibenzo-*p*-dioxin (TCDD), a high-affinity ligand, initiates the expression of a number of genes including P450 enzymes (Cyp 1a1 and Cyp 1b1) [20].

CSC-like cells from the human choriocarcinoma cell line JEG-3 were isolated and identified in this study [21]. The study aimed to examine the effect of functional AhR on the development of CSC-like cells, identify their characteristics, and verify the molecular mechanisms.

Materials and methods

Cell culture

Human choriocarcinoma cell lines (JEG-3, BeWo) were acquired from the American Type Culture Collection (VA, USA). Choriocarcinoma cell lines were cultivated in DMEM with high glucose, 10% fetal bovine serum (FBS), and penicillin/streptomycin and grown in a humidified atmosphere containing 5% CO_2 at 37°C. The culture media and FBS were purchased from Gibco (CA, USA).

TCDD (AccuStandard, USA) and XAV-939 (Selleckchem, TX, USA) were stocked and prepared fresh just prior to each experiment in DMSO, whereas the DMSO concentration did not exceed 0.1%. Live cells were treated with control media (0.1% DMSO) or 10 nM TCDD for 48 h for corresponding experiments.

Spheroid-formation assay

Choriocarcinoma cells were treated as earlier, plated in ultra-low attachment plates at a cell density of 10^4 cells/mL, and grown in serum-free culture medium comprising DMEM/F12 basal medium supplemented with B27 1:50, 20 ng/mL EGF (PeproTech, USA), 20 ng/mL bFGF (PeproTech, USA), and 0.4% bovine serum albumin (BSA). The spheroids were counted under a microscope.

Colony formation and soft agar clonogenicity assay

The supernatant spheres were collected, centrifuged at 500 rpm for 5 min, cultured in low-adhesion six-well plates (5–10 cells/well) in 100 μL of serum-free culture medium as described earlier. Then, 10 μL of the medium was added every day until the colonies were observed.

The JEG-3 cells and spheres were trypsinized and suspended at a density of 10^3 cells/well in the serum-supplemented or serum-free medium containing 0.3% agar (Sigma–Aldrich). The bottom layer of the well comprised a solidified medium containing 0.6% agar. Colonies > 0.1 mm in diameter were scored. The colony-forming efficiency was calculated by dividing the number of colonies by the number of inoculated cells.

RNA extraction and quantitative real-time PCR (qRT-PCR)

Total RNA was extracted using TRIzol reagent (Invitrogen, USA) and was reverse transcribed into cDNA using cDNA Reverse Transcription kit (TaKaRa, Japan) according to the manufacturer's protocol. qRT-PCR was performed using the SYBR Premix ExTaq (TaKaRa) in an ABI 7500 Real-time PCR System (Thermo, MMAS, USA). The expression levels of genes were calculated using the following equation: fold change = $2^{-\Delta\Delta Ct}$, where Ct represents the threshold cycle for each transcript. $\Delta Ct = Ct_{(target)} - Ct_{(GAPDH)}$ and $\Delta\Delta Ct = \Delta CT_{(treated)} - \Delta CT_{(control)}$

The primers used are listed in supplementary materials.

Flow cytometry

The samples were suspended and labeled with antibodies (BD, CA, USA) following the manufacturer's protocol and tested using a flow cytometer (BD) to assess the surface expression of CD44 and CD133.

Chemotherapy resistance assay

Choriocarcinoma cells or treated cells were seeded into 96-well plates at a density of 10^4cells/well and incubated with methotrexate (MTX, 5 μg/mL) and etoposide (VP16, 10 μg/mL) to measure the chemosensitivity of cells. After being cultured under different experimental conditions, each well was incubated with 10 μL of Cell Counting Kit-8 (CCK-8) (Dojindo, Kumamoto, Japan) for 2 h at 37°C. The absorbance

at 450 nm was measured using a microplate reader (BioTek, VT, USA).

Western blot analysis

The cells were lysed, and total proteins were extracted using RIPA buffer (Beyotime Biotechnology, Shanghai, China). The protein concentration was then quantified by the standard bicinchoninic acid (BCA) method. Equal amounts of protein were loaded onto a gel for sodium dodecyl sulfate–polyacrylamide gel electrophoresis (SDS-PAGE) and transferred to polyvinylidene difluoride (PVDF) membranes (Merck, Darmstadt, Germany). Nonspecific binding sites were blocked using Tris-buffered saline with Tween 20 supplemented with 5% nonfat milk for 1 h at room temperature, and the blot was incubated with specific antibodies at 4°C overnight. After washing, the blot was incubated with an appropriate secondary antibody for 1 h at room temperature, detected with enhanced chemiluminescence reagent (Millipore, MA, USA), and then exposed using chemiluminescence system (Syngene, Cambridge, UK).

Immunofluorescence assay

The cells were grown on glass slides, fixed with 4% paraformaldehyde for 10 min, permeabilized in 0.5% Triton X-100 for 10 min, and blocked with 2% BSA at room temperature for 1 h. Next, they were incubated with each primary antibody overnight at 4°C, followed by FITC-conjugated secondary antibodies for 1 h at room temperature in the dark. Finally, they were counterstained with DAPI, which is a fluorescent stain for nuclear DNA. The fluorescence staining intensity and intracellular localization were then examined using a fluorescence microscope (Leica, Wetzlar, Germany).

Transfection

Choriocarcinoma cells were seeded in 24-well plates at a density of 4×10^4 cells/well and transfected with appropriate concentrated lentivirus AhR short hairpin RNAs for gene silencing and nontarget control shRNA in the presence of polybrene (2.5 μg/mL). The stably transfected cells were selected with puromycin (1 μg/mL). All lentiviruses were provided by GeneChem (Shanghai, China).

Cell proliferation assay

Cell proliferation ability was assessed by the CCK-8 Reagent. Transfected cells and control cells were seeded into the 96-well plates. After being cultured for 48 h, CCK-8 reagent was added into each well and further incubated for 2 h at 37°C. The absorbance at 450 nm was measured using a microplate reader.

Luciferase assay

JEG-3 cells were plated in 12-well plates and co-transfected with a reporter plasmid that contained a reporter construct (wild AhR-ABCG2-binding sites or mutant type), which was purchased from RiboBio Company (Guangzhou, China); shAhR; or TCDD (10 nM). The luciferase activity was determined according to the manufacturer's protocol (Luciferase Assay System, Promega, WI, USA) and measured using GloMax-multimode reader (Promega).

Chromatin immunoprecipitation assay

JEG-3 cells were treated with TCDD (10 nM) for 48 h to induce AhR activation and then cells were collected and fixed in 1% formaldehyde for 10 min at room temperature. Chromatin were sonicated and immunoprecipitated with anti-AhR antibodies (ab2769, Abcam) or nonspecific immunoglobulin G (IgG) antibodies (Life Technologies) using the MAGnify Chromatin Immunoprecipitation System (Invitrogen, Life Technologies). The co-immunoprecipitated DNA fragments and input DNA were amplified by PCR. The primers of ABCG2 used in PCR are listed in supplementary materials.

Xenograft tumorigenicity assay

Female BALB/c mice (aged 6–8 weeks, weighing 18–22 g), obtained from the Shanghai Laboratory Animal Center of the Chinese Academy of Sciences (Shanghai, China), were housed under specific pathogen-free conditions. For cancer cell xenograft experiments, treated cells or parental cells (1×10^7) were resuspended in 50 μL of Matrigel solution (1:1 dilution with DMEM) and injected subcutaneously into the left flanks of the mice ($n = 5$ per group), as described earlier. The tumor volumes were calculated every 5 days and

tumor weights were finally measured. The tumor volumes (mm^3) were calculated as (length × width-^{2})/2. Animal experiments conformed to the protocols approved by the Animal Ethics Committee of Central South University.

Immunohistochemistry assay

Immunohistochemistry (IHC) analysis was performed on formalin-fixed and paraffin-embedded tumors, which were removed from the mice. Antigen retrieval was performed in a citrate buffer. Tissue sections were stained with the indicated primary antibodies at 4°C overnight and secondary antibodies (ZSGB-BIO, Beijing, China) at room temperature for 30 min. The color was developed with the peroxidase substrate DAB at room temperature for 2 min. The slides were observed using a fluorescence microscope. The degree of immunostaining was based on the intensity of staining: 0 (no staining), 1 (weak staining = light yellow), 2 (moderate staining = yellow brown), and 3 (strong staining = dark brown). Further, 2 and 3 were defined as positive, while 0 and 1 were defined as negative.

Statistical analysis

The SPSS software package 17.0 was used for statistical analysis. Continuous data were compared using the Student's *t* test or one-way ANOVA

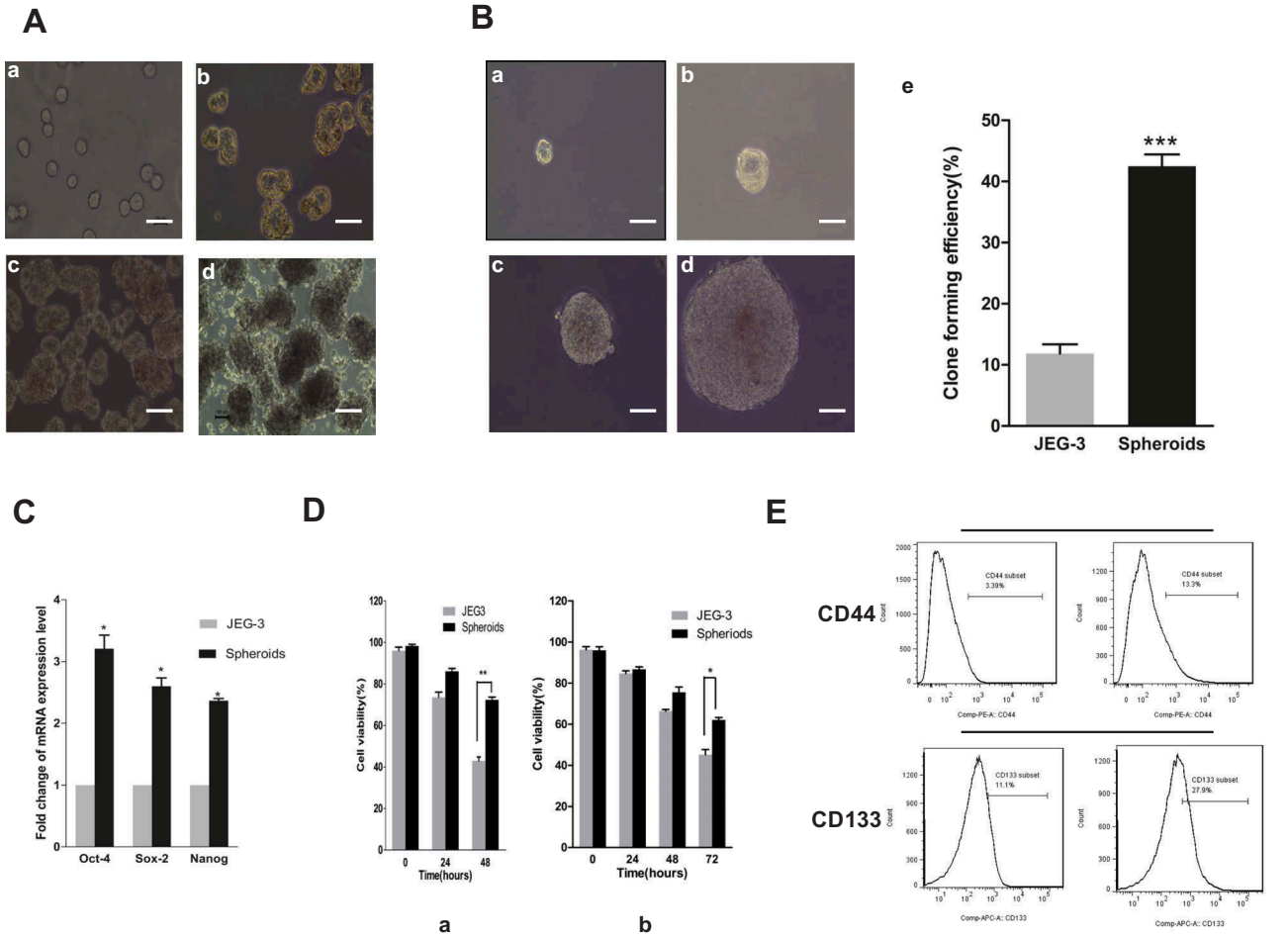

Figure 1. Spheroid cells had stem cell–like characteristics. (a) Images of the spheroids generated from adherent JEG-3 cells were shown from day 0 to day 6 cultured in serum-free media. Scale bar, 100 μm. (a) Day 0, (b) day 2, (c) day 4, and (d) day 6. (b) Clonogenicity of spheroids and adherent cells. Images of a single spheroid cell cultured in serum-free media were shown. (a) Day 1, (b) day 3, (c) day 5, (d) day 7, and (e) quantitation of colony-forming capabilities. (c) Stemness-related genes were examined using RT-PCR. (d) Drug resistance: spheroids and adherent cells were incubated with MTX (left) or VP16 (right), and the viability was measured using CCK-8 assay. (e) Flow cytometric analysis of the surface expression of CD44 and CD133. Each bar represents mean ± SD of three independent experiments. *$P < 0.05$, **$P < 0.01$, ***$P < 0.001$.

analysis. All results were presented as mean ± standard deviation (SD). $P < 0.05$ was considered statistically significant.

Results

Spheroids isolated from human choriocarcinoma JEG3 cells had CSC properties

JEG-3 human choriocarcinoma cells were seeded on low-attachment culture plates in serum-free culture media. Because of serum starvation, some cells died and aggregates of cells were formed, which continued to grow in suspension (Figure 1(a)). The expression levels of stemness-related genes, such as Sox2, Oct4, and Nanog, in the adherent JEG-3 cells and in spheroids were compared to determine whether the spheroids exhibited stem-cell-like characteristics. The levels were analyzed using quantitative (Q)-PCR. The results showed that the mRNA levels of the aforementioned genes were higher in spheroids than in JEG-3 cells (Figure 1(c)). Furthermore, the expression of stem cell markers-CD44 and CD133 were evaluated by flow cytometry analysis. The results showed that the spheroids expressed higher levels of these markers, too (Figure 1(e)). When a single spheroid cell was cultured in isolation in the serum-free media, a colony was formed. Therefore, the clonogenicity of spheroids and JEG-3 cells was compared, which suggested that the former had a stronger clone-forming efficiency than the latter (Figure 1 (b)). Furthermore, when comparing other CSC characteristics, the spheroid cells showed higher proliferation rate and higher resistance to MTX

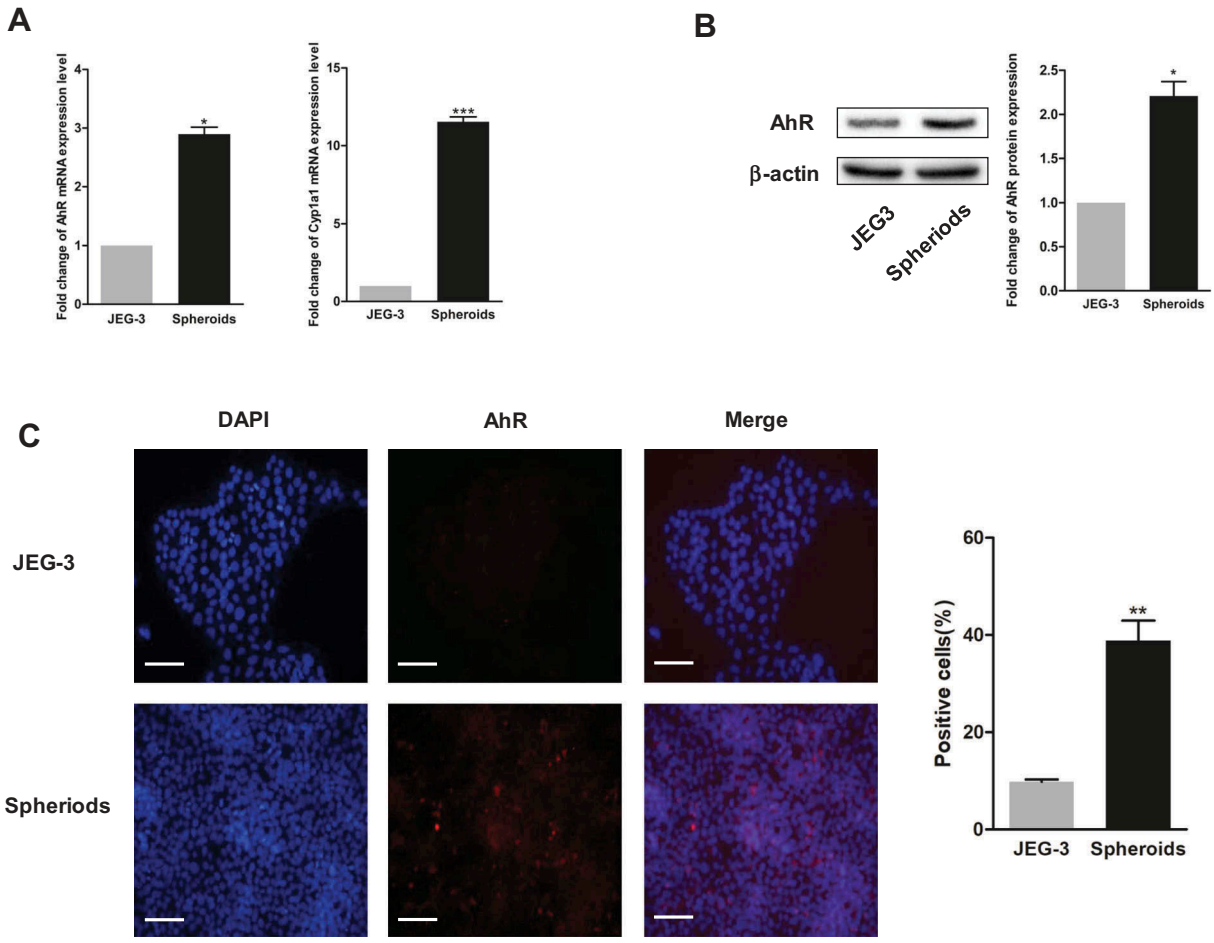

Figure 2. Expression of AhR increased in spheroids. (a) RT-PCR analysis of the mRNA expression of AhR (left) and Cyp1A1 (right) in spheroids and adherent cells. (b) Expression of AhR detected using Western blot analysis was shown (left). Respective change was depicted as fold change and β-actin served as the loading control (right). (c-d) Expression and localization of AhR in the spheroids and JEG-3 cells were shown by immunofluorescence. The percentage of AhR-positive cells was increased in the spheroid group compared to the adherent group. Scale bar, 100 μm. Each bar represents mean ± SD of three independent experiments. *$P < 0.05$, **$P < 0.01$, ***$P < 0.001$.

and VP16 (Figure 1(d)). All of these results suggested that the spheroid cells had CSC characteristics.

Ahr was activated and highly expressed in the CSC populations

The mRNA expression levels of AhR and an AhR target gene, Cyp 1a1, were quantified to examine the level of AhR expression in spheroid cells and adherent cells. Figure 2(a) shows that the basal expression levels of AhR mRNA were higher in spheroids than in JEG-3 cells by approximately threefold and Cyp 1a1 mRNA levels were higher by tenfold. When examining the expression levels of AhR in spheroids using Western blotting analysis, higher expression of AhR was observed in spheroids than in JEG-3 cells (Figure 2(b)). Further analysis of the activation of AhR in spheroids versus JEG-3 cells using immunofluorescence assay revealed higher AhR content and localization (red) in spheroids (Figure 2(c)). These results showed the importance of AhR in CSCs.

Effects of ahr activation and inhibition on cell proliferation, drug resistance and spheroid formation

Based on the data from Q-PCR, Western blot analysis, and immunofluorescence assays, this study investigated whether AhR regulated CSC properties in choriocarcinoma. We stably knockdown the expression of AhR in JEG-3 and BeWo cells by AhR shRNA. The mRNA and protein level of AhR were dramatically reduced after transfection in both JEG-3 and BeWo cells (shAhR) (Figure 3(a,b)). At the same time, choriocarcinoma cells were treated

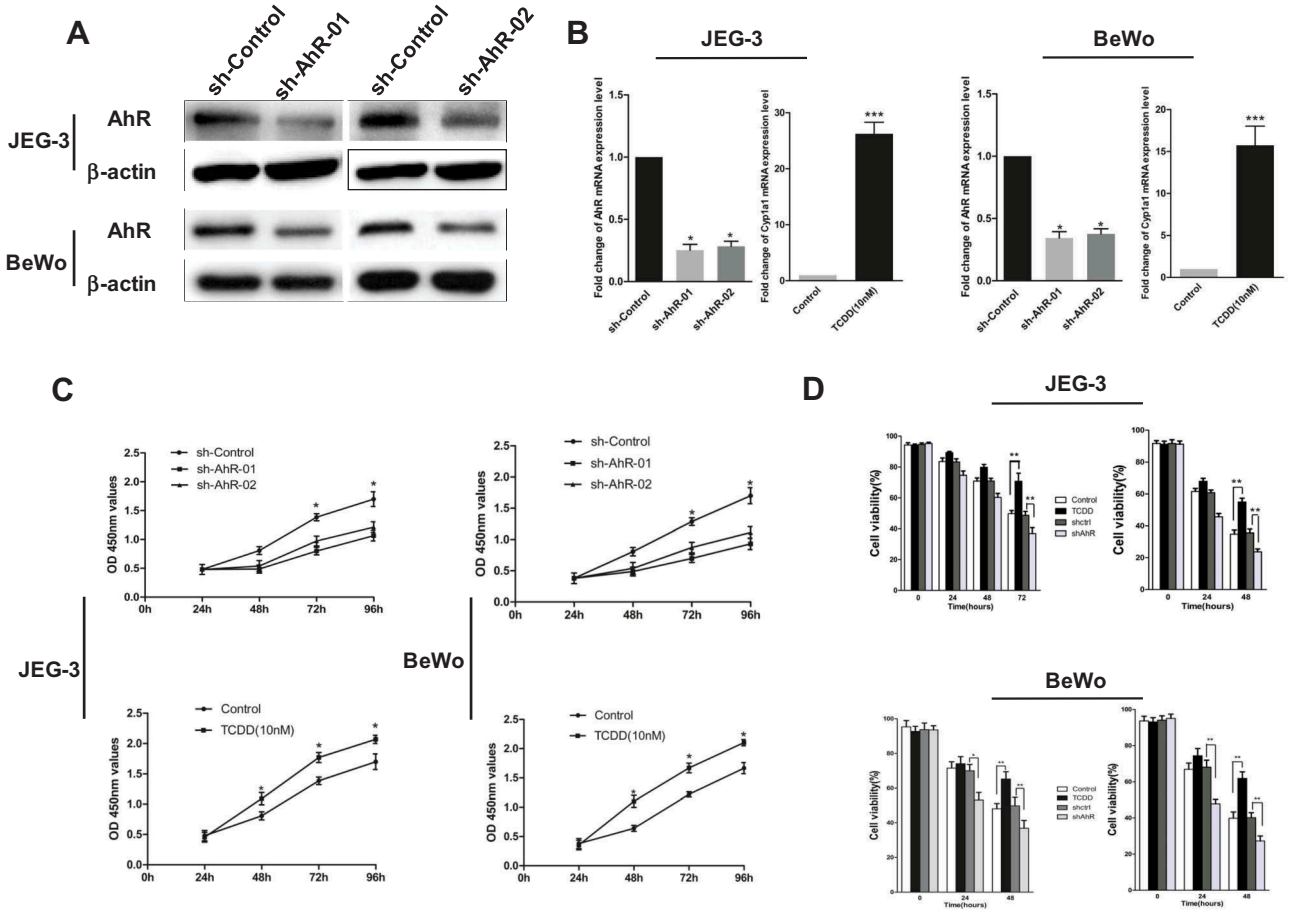

Figure 3. AhR regulated cell proliferation and drug resistance of choriocarcinoma cells. (a) AhR expression was significantly downregulated in JEG-3 and BeWo cells by transfection of AhR shRNA. (b) RT-PCR analysis of AhR and Cyp1A1 expression levels in JEG-3 and BeWo cells transduced with AhR shRNA or treated with TCDD. (c) Cell viability of JEG-3 and BeWo cells quantified by using CCK-8 assays. (d) The viability of JEG-3 and BeWo cells with or without AhR knockdown (shAhR) or TCDD treatment was measured by CCK-8 assay after treatment of cells with indicated concentrations of MTX(left) or VP16 (right). Each bar represents mean ± SD of three independent experiments. *$P < 0.05$, **$P < 0.01$, ***$P < 0.001$.

with TCDD (10 nM), a well-known AhR agonist, for 48 h. Higher expression levels of AhR in the nucleus and mRNA level of Cyp1a1 were observed (Figure 3 (b)) in the treated cells. CCK-8 assay indicated that AhR knockdown significantly inhibited cell proliferation of both JEG-3 and BeWo cells compared to corresponding negative control (shControl), whereas, TCDD treatment promoted cell proliferation (Figure 3(c)). In addition, the study tested whether the expression of AhR regulated chemoresistance. Knockdown of the expression of AhR in both JEG-3 cells and BeWo cells decreased the viability after treatment with chemotherapeutic agents such as MTX or VP16 compared with the controls, indicating a significant increase in the drug sensitivity. On the contrary, the activation of AhR after TCDD treatment increased the drug sensitivity (Figure 3(d)). Together, these results suggested the involvement of AhR in the regulation of chemoresistance in choriocarcinoma cells.

Next, the effects of AhR activation by TCDD and AhR inhibition by knockdown on spheroid formation, as an indicator of an increase or decrease in the self-renewal capacity of choriocarcinoma cells, were examined. Captured images and data showed that the sphere-forming ability increased when AhR was activated. In contrast, the knockdown of AhR resulted in a significant decrease in the number and size of the spheroids (Figure 4). This result suggested that AhR might regulate CSC properties in choriocarcinoma cells.

Ahr knockdown suppressed tumorigenesis in vivo

To confirm the functional role of AhR in tumor growth of choriocarcinoma *in vivo*, a xenograft

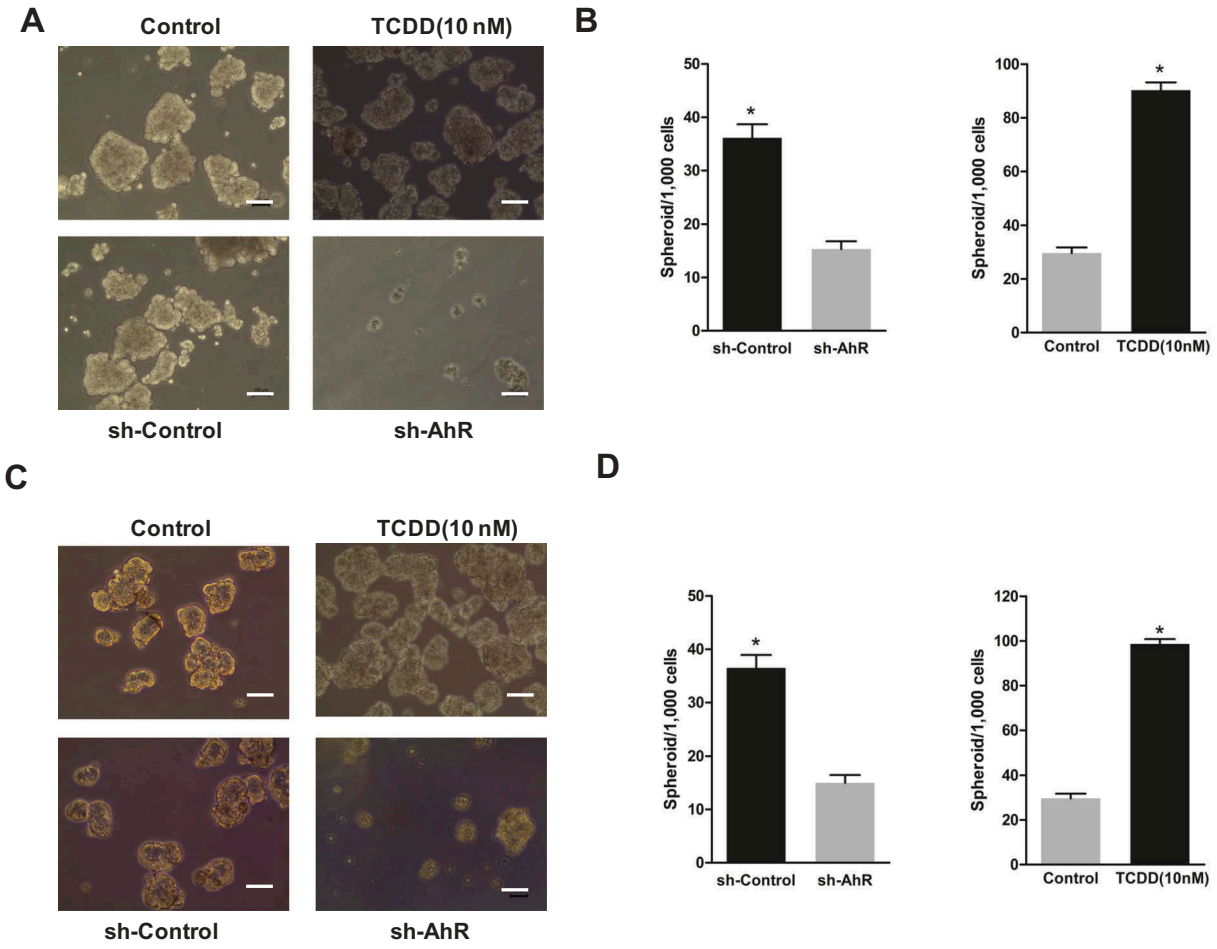

Figure 4. AhR promoted the spheroid formation. (a) Images of spheroids from JEG-3 cells with or without AhR activation (upper) or knockdown (lower) were shown. (b) The spheroids generated from 1000 cells of JEG-3 cells with or without TCDD treatment (right) and with or without AhR knockdown (left) were shown. (c) Images of spheroids from BeWo cells with or without AhR activation (upper) or knockdown (lower) were shown. (d) The spheroids generated from 1000 cells of BeWo cells with or without TCDD treatment (right) and with or without AhR knockdown (left) were shown. Data are presented as mean ± SD from three independent experiments. *$P < 0.05$.

model was established in BALB/c nude mice. AhR shRNA or negative control stably transfected JEG-3 cells were injected. After 30 days, the xenograft tumor of shAhR group were smaller in size (Figure 5(a,c)) and lighter in tumor weight (Figure 5(b)) compared with negative control group. The results showed that AhR knockdown generated much smaller tumors. At the same time, IHC of the tumor tissues showed the relative AhR and ABCG2 expression were significantly lower in AhR shRNA group (Figure 5(d)). These results suggested that AhR knockdown suppressed the growth of JEG-3 cells *in vivo*.

Ahr regulated ABCG2 via directly binding and transcriptional activation

ABCG2 is present on the plasma membrane of many types of human cancer cells and has an important role in the multidrug resistance during chemotherapy. The present study confirmed the involvement of ABCG2 in the development of CSC characteristics. Spheroid cells were found to have higher mRNA and protein expression levels of ABCG2 compared with JEG-3 cells (Figure 6(e,f)). Interestingly, the expression of ABCG2 was affected by AhR. The expression levels of mRNA and protein of ABCG2 increased after AhR was activated by TCDD (Figure 6(c,d)). Therefore, AhR-binding site in ABCG2 was searched and the reporter assay was performed with the promoter of ABCG2 after cotransfection of reporter constructs with shAhR or TCDD treatment so as to examine whether AhR directly regulated ABCG2. The relative luciferase activity significantly decreased with transfection of shAhR, but it increased on TCDD stimulation (Figure 6(a)). These differences became diminished when the AhR-binding sites on ABCG2 was mutated (supplementary materials). Next, we used chromatin immunoprecipitation-PCR experiment with anti-AhR antibody to further assess if AhR could directly bind to the ABCG2 promoter

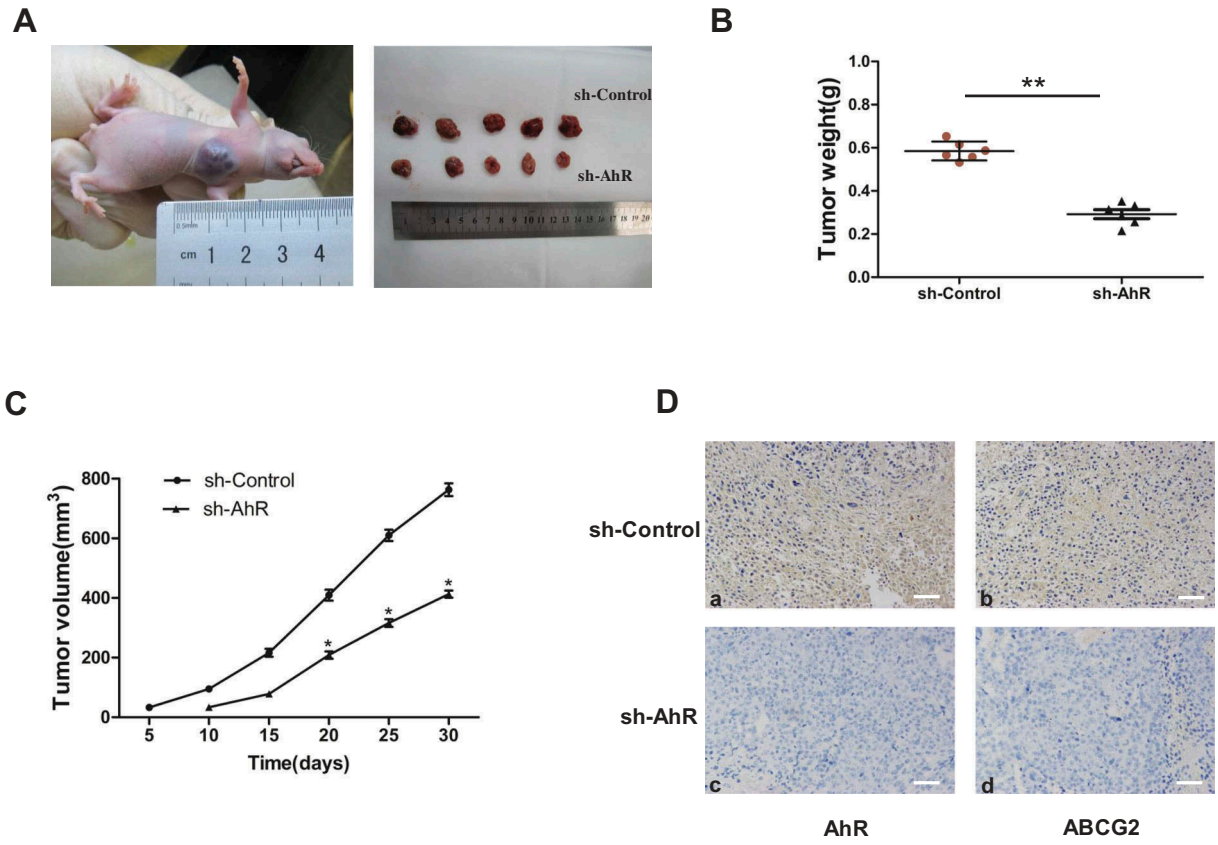

Figure 5. AhR knockdown suppressed tumorigenesis in vivo. (a) Representative image of mice on day 35 after injection of JEG-3 cells is shown. The sizes of resected tumors removed from mice on day 35 after injection of JEG-3 cells with or without AhR knockdown into nude mice were show. (b) Comparison of excised tumors weight in two groups. (c) Tumor size was measured on the indicated day after injection of corresponding cells into nude mice. (d)Tissues of every group were collected and stained with antibody against AhR (left) and ABCG2 (right) for IHC assays. Each bar represents mean ± SD ($n = 6$). *$P < 0.05$, **$P < 0.01$.

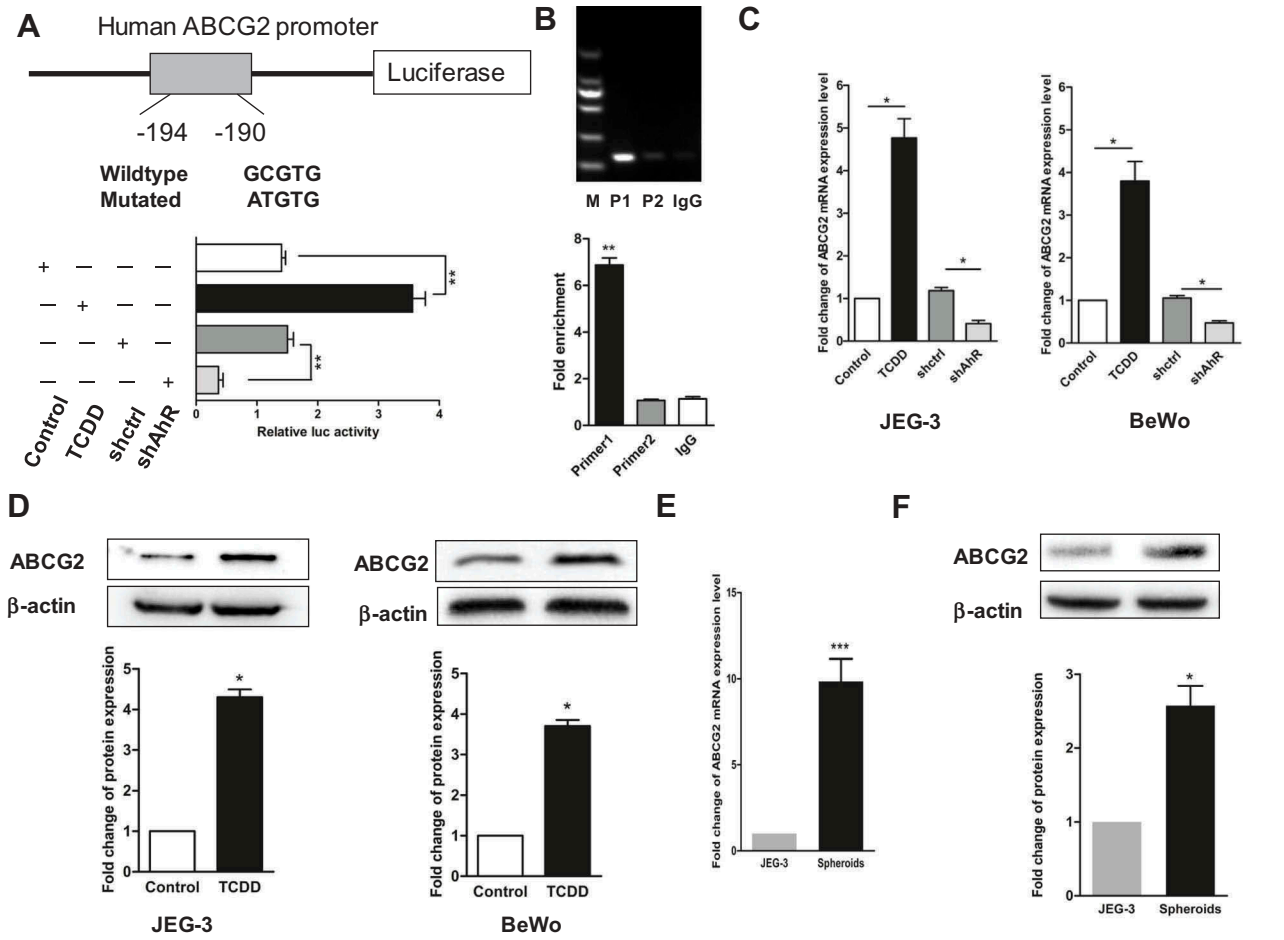

Figure 6. AhR transcriptionally activated ABCG2. (a) AhR-binding sites in ABCG2 promoter were marked with a box. Luciferase reporter assay was performed in JEG-3 cells transfected with shAhR or treated with TCDD and controls. (b) ChIP analysis of AhR binding to the ABCG2 promotor in the JEG-3 cells. qPCR was performed with primer specific to regions around the AhR-binding motifs (P1) and a control region (P2). (c) RT-PCR analysis of the ABCG2 level in JEG-3 cells (left) and BeWo cells (right) with AhR knockdown or activation compared with controls. (d) Western blot analysis results of JEG-3 (left) and BeWo (right) cells with or without AhR activation were shown. (e) RT-PCR analysis of the mRNA expression of ABCG2 in spheroids and JEG-3 cells. (f) Expression of ABCG2 detected in two groups using Western blot analysis was shown. Each bar represents mean ± SD of three independent experiments. *$P < 0.05$, **$P < 0.01$, ***$P < 0.001$.

region in JEG-3 cells. Result showed that ABCG2 was enriched in AhR immunoprecipitate compared with control IgG immunoprecipitate (Figure 6(b)). These data demonstrated that ABCG2 was a direct of the transcription factor AhR.

Wnt/β-catenin pathway might be involved in ahr-mediated effects on CSC characteristics

Choriocarcinoma cells were treated with TCDD (10 nM) in the presence and absence of an inhibitor of Wnt/β-Catenin (5 μM) to explore whether the Wnt signaling pathway, which is an important pathway in CSC development, was involved in the AhR activation mediating CSC characteristics. Similarly, the spheroids were counted and data showed that the number of spheroids decreased on treating the cells with the inhibitor XAV-939 and TCDD, compared with TCDD treated alone (Figure 7(a)). Then, the effect of AhR activation on the protein expression level of β-catenin was examined. Western blot analysis showed that TCDD induced the expression of β-catenin as well as CyclinD1and c-MYC (β-catenin downstream targets) (Figure 7(b)). Finally, the effect of AhR activation and inhibition on the expression of β-catenin and nuclear translocation in JEG-3 cells was assessed using immunofluorescence assay. Images showed that TCDD increased while shAhR decreased the expression and nuclear translocation of β-catenin (red) (Figure 7(c,d)) compared with the controls. Taken together, these

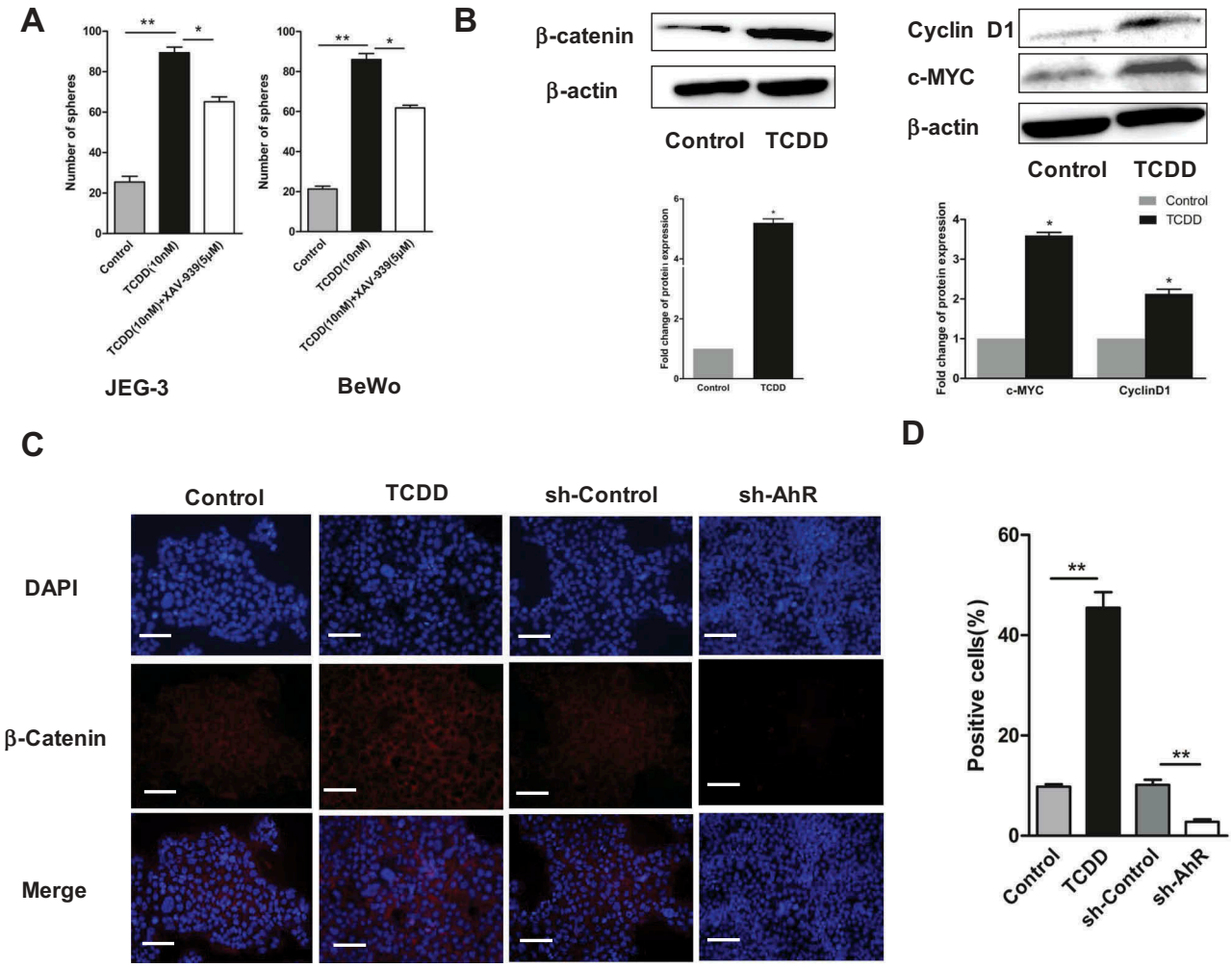

Figure 7. Wnt/β-Catenin pathway might be involved in AhR-mediated effects on CSC characteristics. (A) JEG-3 and BeWo cells were treated with TCDD in the presence and absence of Wnt inhibitor (XAV-939). The spheroids were counted. (B) The expression of β-catenin, Cyclin D1 and c-MYC (two β-catenin downstream targets) in JEG-3 cells treated with TCDD were determined using Western blot analysis. (C-D) JEG-3 cells treated with TCDD or stably transfected with AhR shRNA were stained with primary antibodies against β-catenin (red) followed by secondary antibodies and DAPI (blue). Then, β-catenin localization and nuclear translocation were determined using immunofluorescence assay. The percentages of β-catenin -positive cells in different groups were shown. Data are presented as mean ± SD from three independent experiments. *$P < 0.05$, **$P < 0.01$.

results suggested the possible involvement of Wnt pathway in the effects of AhR on CSCs.

Discussion

In this study, CSCs were isolated from the human choriocarcinoma cell line JEG-3 through spheroid formation, which is a defining characteristic of epithelial stem cells [22–24]. The study first reported the choriocarcinoma CSCs. These floating spheres also overexpressed stem cell–related genes (Oct-4, Nanog, and Sox-2) and stem cell markers (CD133 and CD44) and had strong proliferative and invasive abilities. Increasing evidence suggested that the activation of AhR dramatically increased the development of CSCs [25–27]. All these results suggested that AhR facilitated tumorigenesis in part through the maintenance of cells with CSC characteristics. On the contrary, AhR was also reported to act as a potential tumor suppressor [28–30]. This study found that the expression of AhR was significantly higher in spheroids than in adherent cells, suggesting that AhR might function as an oncogene in choriocarcinoma.

To test the hypothesis, this study investigated the expression of AhR-regulated gene CYP1A1 and AhR cellular localization, which represented the level of AhR activity in the spheroids versus adherent cells. The results showed that the basal expression of

CYP1A1 mRNA and AhR nuclear localization were markedly higher in spheroids than in adherent non-CSCs of choriocarcinoma. The activation of AhR promoted the CSC-like characteristics, including spheroid population, cell proliferation, chemoresistance, and tumorigenic potential. In contrast, the knockdown of AhR decreased these abilities. In addition, Wnt/β-catenin signaling pathway is known to contribute to CSC development and maintenance while being critically important in CSC biology, which has been demonstrated in many studies [31–33]. The present study showed that AhR probably controlled β-catenin activation. Importantly, recent investigations have shown that chemotherapy resistance is a more meaningful marker of metastasis [34]. AhR-mediated drug resistance has an even greater significance. Previous studies associated the AhR activation with ABCG2-mediated resistance to drugs [35,36]. It has been reported that AhR is a transcriptional activator of ABCG2 [37]. Hence, it was concluded that AhR was involved in the overexpression of ABCG2 in spheroid cells, indicating that it was a crucial regulator of chemoresistance in choriocarcinoma.

In summary, this novel study revealed that AhR promoted CSC-like characteristics in choriocarcinoma and might be a target for novel therapeutics.

Disclosure statement

No potential conflict of interest was reported by the authors.

Funding

This work was supported by the Natural Science Foundation of China (No.81472434).

References

[1] Powles T, Savage PM, Stebbing J, et al. A comparison of patients with relapsed and chemo-refractory gestational trophoblastic neoplasia. Br J Cancer. 2007;96(5):732–737. PMID: 17299394. .

[2] Seckl MJ, Sebire NJ, Fisher RA, et al. Gestational trophoblastic disease: ESMO clinical practice guidelines for diagnosis, treatment and follow-up. Ann Oncol. 2013;10(24):39–50. PMID: 23999759.

[3] Soper JT, Evans AC, Conaway MR, et al. Evaluation of prognostic factors and staging in gestational trophoblastic tumor. Obstet Gynecol. 1994;84(6):969–973. PMID:7970479.

[4] Taylor F, Short D, Winter MC, et al. A retrospective study to evaluate single agent methotrexate treatment in low risk gestational choriocarcinoma in the United Kingdom. Gynecol Oncol. 2015;136:258–263. PMID:25542400. .

[5] Gilani MM, Fariba B, Behtash N, et al. The WHO score predicts treatment outcome in low risk gestational trophoblastic neoplasia patients treated with weekly intramuscular methotrexate. J Cancer Res Ther. 2013;9:38–43. PMID:23575072. .

[6] Ngan HY. The practicability of FIGO 2000 staging for gestational trophoblastic neoplasia. Int Gynecol Cancer. 2004;14:202–205. PMID:15086715. .

[7] Bonnet D, Dick JE. Human acute myeloid leukemia is organized as a hierarchy that originates from a primitive hematopoietic cell. Nat Med. 1997;3:730–737. PMID:9212098. .

[8] Clarke MF, Dick JE, Dirks PB, et al. Cancer stem cells—perspectives on current status and future directions: AACR Workshop on cancer stem cells. Cancer Res. 2006;66:9339–9344. PMID:16990346. .

[9] AI-Hajj M, Wicha MS, Benito-Hernandez A, et al. Prospective identification of tumorigenic breast cancer cells. Proc Natl Sci USA. 2003;100:3983–3988. PMID:12629218. .

[10] Singh SK, Hawkins C, Clarke ID, et al. Identification of human brain tumour initiating cells. Nature. 2004;432:396–401. PMID:15549107. .

[11] Ricci-Vitiani L, Lombardi DG, Pilozzi E, et al. Identification and expansion of human colon-cancer-initiating cells. Nature. 2007;445:111–115. PMID:17122771. .

[12] Ho MM, Ng AV, Lam S, et al. Side population in human lung cancer cell lines and tumors is enriched with stem-like cancer cells. Cancer Res. 2007;67:4827–4833. PMID:17510412. .

[13] Abdullah LN, Chow EK. Mechanisms of chemoresistance in cancer stem cells. Clin Transl Med. 2013;2:3. PMID:23369605. .

[14] Bomken S, Fisher K, Heidenreich O, et al. Understanding the cancer stem cell. Br J Cancer. 2010;103:493–495. PMID:20664590. .

[15] Reya T, Morrison SJ, Clarke MF, et al. Stem cells, cancer, cancer stem cells. Nature. 2001;414:105–111.

[16] Winquist RJ, Furey BF, Boucher DM. Cancer stem cells as the relevant biomass for drug discovery. Curr Opin Pharmacol. 2010;10:385–390. PMID:20630801. .

[17] Kewley RJ, Whitelaw ML, Chapman-Smith A. The mammalian basic helix-loop-helix/PAS family of transcriptional regulators. Int J Biochem Cell Biol. 2004;36:189–204. PMID:14643885. .

[18] Kerzee JK, Ramos KS. Constitutive and inducible expression of Cyp1a1 and Cyp1b1 in vascular smooth muscle cells: role of the Ahr bHLH/PAS transcription factor. Circ Res. 2001;89(7):573–582. PMID:11577022.

[19] Safe S, Lee SO, Jin UH. Role of the aryl hydrocarbon receptor in carcinogenesis and potential as a drug target. Toxicol Sci. 2013;135:1–16. PMID:23771949. .

[20] Pollenz RS. The mechanism of AH receptor protein down-regulation (degradation) and its impact on AH receptor-mediated gene regulation. Chem Biol Interact. 2002;141:41–61. PMID:12213384. .

[21] Cai JT, Peng TF, Liu HN, et al. Isolation, culture and identification of choriocarcinoma stem-like cells from the human choriocarcinoma cell-line JEG-3. Cell Physiol Biochem. 2016;38:1421–1432. PMID:27606814. .

[22] Choi EJ, Seo EJ, Kim DK, et al. FOXP1 functions as an oncogene in promoting cancer stem cell-like characteristics in ovarian cancer cells. Oncotarget. 2016;7:3506–3519. PMID:26654944. .

[23] Huso TH, Resar LM. The high mobility group A1 molecular switch: turning on cancer – can we turn it off? Opin Ther Targets. 2014;18:541–553. PMID:24684280. .

[24] Seo EJ, Kwon YW, Jang IH, et al. Autotaxin regulates maintenance of ovarican cancer stem cells through lysophosphatidic acid – mediated autocrine mechanism. Stem Cells. 2016;34:551–564. PMID:26800320. .

[25] Standford EA, Wang Z, Novikov O, et al. The role of the aryl hydrocarbon receptor in the development of cells with the molecular and functional characteristics of cancer stem – like cells. BMC Biol. 2016;14:20. PMID:26984638. .

[26] Abdullah AD, Alhoshani A, Heshan MK. Aryl hydrocarbon receptor/cytochrome P450 1A1 pathway mediates breast cancer stem cells expansion through PTEN inhibition and β-Catenin and Akt activation. Molecular Cancer. 2017;16:14. PMID:28103884. .

[27] Standford EA, Ramirez-Cardenas, Alejandra, Wang Z., et al. Role for the Aryl hydrocarbon receptor and diverse ligands in oral squamous cell carcinoma migration and tumorigenesis. Mol Cancer Res. 2016;14:696–706. PMID: 27130942. .

[28] Zhao S, Kanno Y, Nakayama M, et al. Activation of the aryl hydrocarbon receptor represses mammosphere formation in MCF-7 cells. Cancer Lett. 2012;317:192–198. PMID:22123295. .

[29] Hall JM, Barhoover MA, Kazmin D, et al. Activation of the aryl-hydrocarbon receptor inhibits invasive and metastatic features of human breast cancer cells and promotes breast cancer cell differentiation. Mol Endocrinol. 2010;24(2):359–369. PMID: 20032195. .

[30] Prud'homme GJ, Glinka Y, Toulina A, et al. Breast cancer stem-like cells are inhibited by a non-toxic aryl hydrocarbon receptor agonist. Plos One. 2010;5:e13831. PMID:21072210. .

[31] Holland JD, Klaus A, Garratt AN, et al. Wnt signaling in stem and caner stem cells. Curr Opin Cell Biol. 2013;25:254–264. PMID:23347562. .

[32] Reya T, Clevers H. Wnt signaling in stem cells and cancer. Nature. 2005;434:843–850. PMID:15829953. .

[33] Bisson I, Prowse DM. WNT signaling regulates self-renewal and differentiation of prostate cancer cells with stem cell characteristics. Cell Res. 2009;19:683–697. PMID:19365403. .

[34] Fischer KR, Durrans A, Lee S, et al. Epithelial-to-mesenchymal transition is not required for lung metastasis but contributes to chemoresistance. Nature. 2015;527:472–476. PMID:26560033. .

[35] Ebert B, Seidel A, Lampen A. Identification of BCRP as transporter of benzo[a]pyrene conjugates metabolically formed in Caco-2 cells and its induction by Ah-receptor agonists. Carcinogenesis. 2005;26(10):1754–1763. PMID:15917307. .

[36] To KK, Yu L, Liu S, et al. Constitutive AhR activation leads to concomitant ABCG2-mediated multidrug resistance in cisplatin-resistant esophageal carcinoma cells. Mol Carcinog. 2012;51(6):449–464. PMID:21678497. .

[37] Tan KP, Wang B, Yang M, et al. Aryl hydrocarbon receptor (AHR) is a transcriptional activator of the human breast cancer resistance protein (BCRP/ABCG2). Mol Pharmacol. 2010;78(2):175–185. PMID:20460431. .